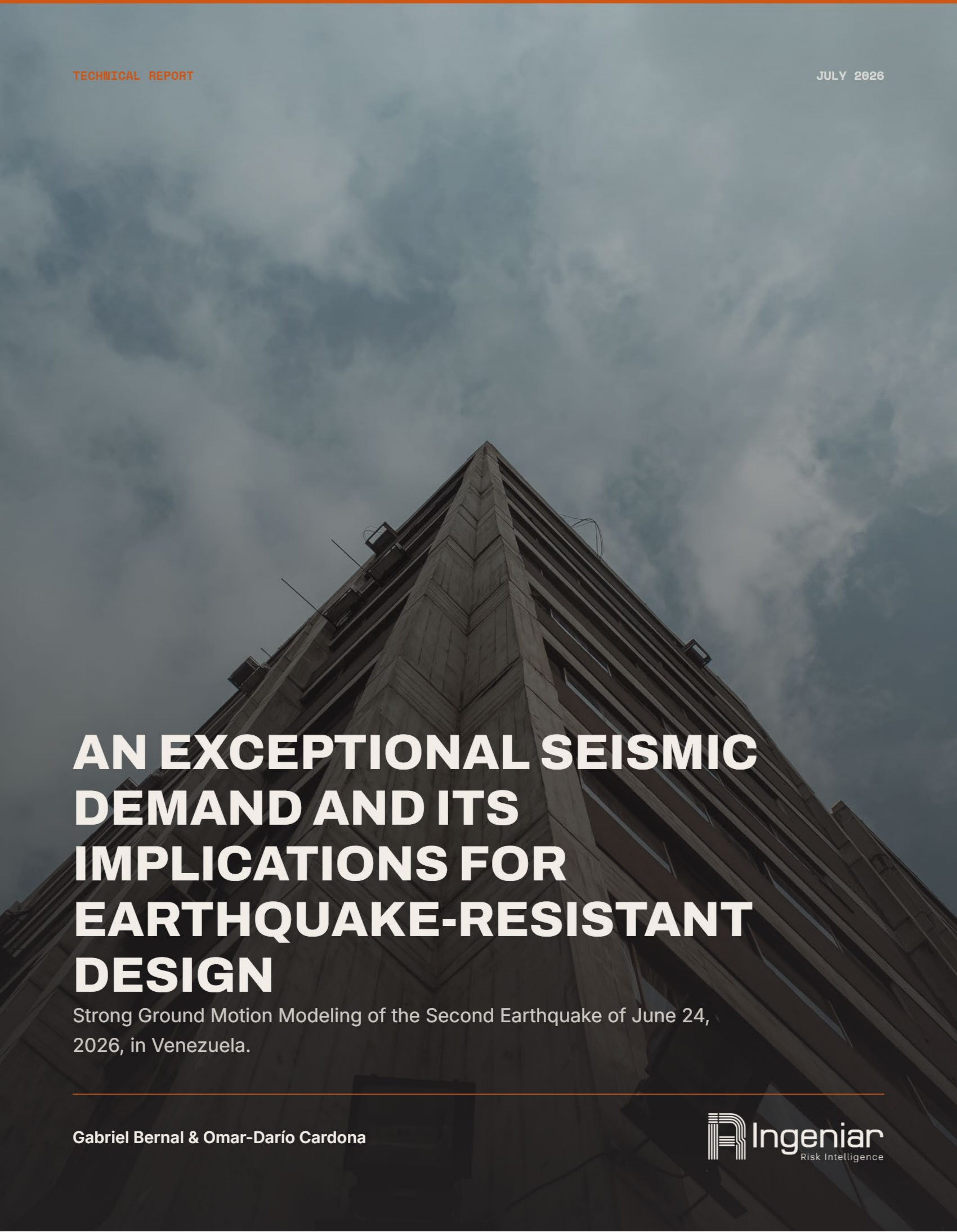

TECHNICAL REPORT

JULY 2026

AN EXCEPTIONAL SEISMIC DEMAND AND ITS IMPLICATIONS FOR EARTHQUAKE-RESISTANT DESIGN

Strong Ground Motion Modeling of the Second Earthquake of June 24, 2026, in Venezuela.

Gabriel Bernal & Omar-Darío Cardona

Ingeniar
Risk Intelligence

AN EXCEPTIONAL SEISMIC DEMAND AND ITS IMPLICATIONS FOR EARTHQUAKE-RESISTANT DESIGN

Strong Ground Motion Modeling of the Second Earthquake of June 24, 2026, in Venezuela

Gabriel Bernal[1] & Omar-Darío Cardona[2]

1 SCOPE OF THE STUDY

This report presents a preliminary assessment aimed at characterizing the strong ground motion generated by the second earthquake of the seismic doublet that struck Venezuela on June 24, 2026, and evaluating, through physics-based modeling, the potential local site amplification effects associated with the geological and geotechnical conditions of the central Venezuelan coast.

Because no strong-motion recordings are currently available for this event, the analysis is based on numerical simulations of the earthquake rupture process, seismic wave propagation, and the dynamic response of representative soil deposits. Consequently, the resulting accelerograms are not instrumental recordings but synthetic ground-motion time histories that are consistent with the currently available seismological information and with established principles of earthquake engineering.

Rather than attempting to reproduce the exact ground motion at a specific location, the objective is to generate representative scenarios that facilitate the interpretation of the severity of the ground shaking, improve the understanding of the mechanisms that may have contributed to the observed damage, and provide a technical basis for future seismic hazard assessments, seismic microzonation studies, updates to design response spectra, and urban planning and resilient reconstruction initiatives.

2 INTRODUCTION

On June 24, 2026, the north-central region of Venezuela was affected by a regionally significant seismic sequence consisting of two major earthquakes that caused extensive damage as well as substantial human and economic losses across large areas of the country. Both events occurred within the tectonic setting associated with the interaction between the Caribbean and South American plates, one of the most important seismogenic systems in northern South America and the primary source of seismic hazard affecting Venezuelan territory.

Although both earthquakes belong to the same seismic sequence and are considered in the overall description of the event, this study focuses primarily on the Mw 7.5 earthquake because of its significance in terms of the strong ground motion it generated and its impact on buildings and infrastructure. The magnitude of the event, its rupture mechanism, and its relative location with respect to the major urban

[1] CSO INGENIAR CAD/CAE Ltda. Assistant Professor. Universidad Nacional de Colombia – Bogotá Campus.
[2] CEO INGENIAR CAD/CAE Ltda. Full Professor. Universidad Nacional de Colombia – Manizales Campus.

centers along Venezuela's central coastline warrant a detailed evaluation of the resulting seismic demand and the potential associated secondary effects.

Estimating the effects of an earthquake of this magnitude requires an explicit characterization of the strong ground motion, recognizing that many geotechnical phenomena and structural damage mechanisms depend not only on simplified intensity measures such as Peak Ground Acceleration (PGA), but also on the complete temporal evolution of the ground motion, its frequency content, effective duration, cumulative energy, and spectral variability. Accordingly, the analyses presented herein are based on simulations of synthetic accelerograms representative of the earthquake, allowing the expected physical characteristics of the ground motion to be reproduced in a physically consistent manner.

To this end, a simplified accelerogram simulation methodology developed by INGENIAR: Risk Intelligence (Bernal et al., 2026) was employed to efficiently generate synthetic strong-motion records that are physically compatible with earthquake rupture processes. The methodology realistically reproduces both the temporal and frequency characteristics of ground-motion records while maintaining high computational efficiency, enabling the generation of multiple realizations of earthquake ground motion for different locations and site conditions. This approach is particularly well suited for rapid post-earthquake seismic hazard and risk assessments following large-magnitude earthquakes.

The first stage of the analysis focuses on characterizing the strong ground motion generated by the Mw 7.5 earthquake, without considering the potential cumulative effects of subsequent aftershocks or the highly unlikely influence of the preceding first event. Based on simulated accelerograms and the corresponding intensity measures, expected levels of seismic demand are evaluated at different locations along the central Venezuelan coast. The study focuses on the urban areas of Catia La Mar, La Guaira, and Caraballeda, owing to their high urban density and the presence of geological conditions susceptible to local site amplification and seismic degradation of near-surface materials.

A site-specific evaluation was subsequently performed for the dynamic response of the alluvial fan deposits that underlie much of the coastal plain in La Guaira State. The analysis considers one-dimensional seismic wave propagation through representative subsurface profiles to estimate the modification of the incoming ground motion and quantify the local site effects that may influence the severity of seismic demand at the ground surface.

The dynamic site response results provide the basis for evaluating the potential occurrence of earthquake-induced soil liquefaction. To this end, the cyclic loading imposed by the simulated strong ground motion is analyzed together with the susceptibility of the alluvial deposits, considering the available geotechnical and stratigraphic information for the study area. This assessment makes it possible to identify sectors potentially exposed to significant reductions in the strength and stiffness of saturated granular soils as a consequence of the seismic excitation generated by the event.

The primary objective of this study is to contribute to a better understanding of the physical processes associated with the earthquake and the mechanisms through which they may translate into damage to buildings, infrastructure, and the built environment. By providing a detailed characterization of the strong ground motion, local site effects, and the potential for earthquake-induced geotechnical hazards, the study seeks to generate technically sound information that enhances current knowledge of the seismic behavior of the region and its implications for disaster risk management. Furthermore, the results are intended to provide technical input for future land-use planning, structural design and retrofitting, emergency response, and disaster risk reduction strategies, thereby contributing to reduced vulnerability and helping prevent future earthquakes of similar characteristics from producing comparable—or even greater—human, social, and economic consequences.

Building upon the seismic demand estimates derived from the simulated strong ground motion, the local site response analyses, and the liquefaction assessment presented in this report, a subsequent study will provide a detailed evaluation of physical damage and economic losses through the application of building vulnerability models and building-specific loss assessment methodologies.

3 DESCRIPTION OF THE EARTHQUAKE

On June 24, 2026, two earthquakes of moment magnitude Mw 7.2 and Mw 7.5 occurred in rapid succession in north-central Venezuela. According to the U.S. Geological Survey (USGS), the rupture initiations were separated by only 38 seconds, and both events had nearly identical epicentral locations. The first earthquake, with magnitude Mw 7.2, has been associated with the Boconó Fault, which trends southeast–northwest and converges near the epicentral area with the San Sebastián Fault. The second event, with magnitude Mw 7.5, has been attributed to the San Sebastián Fault, where rupture propagated predominantly from west to east along a trajectory approximately parallel to the Venezuelan coastline. Figure 1 presents the macroseismic intensity maps estimated by the USGS for both earthquakes.

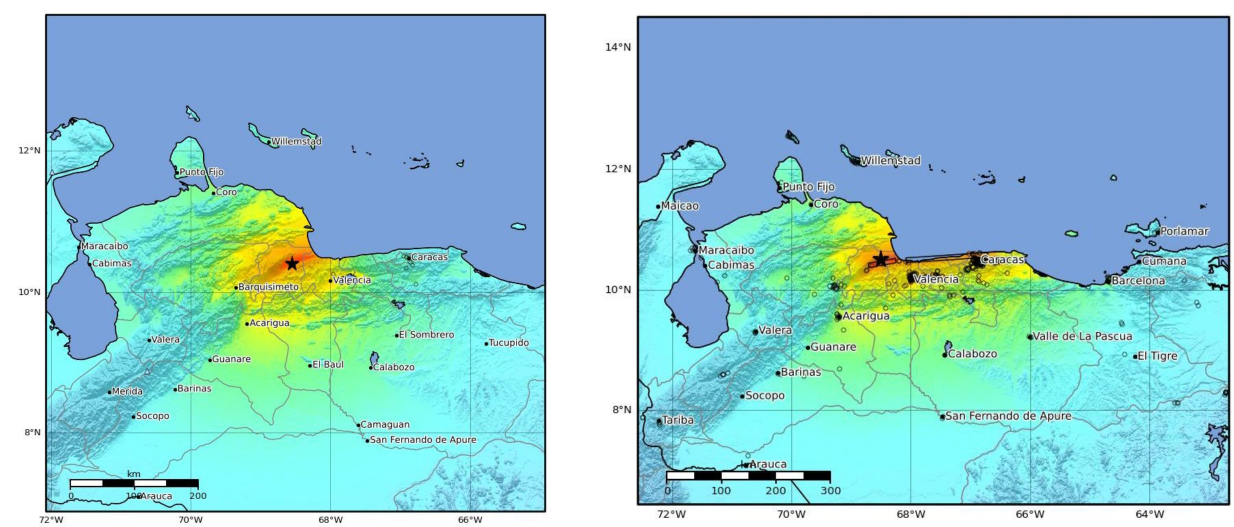

Figure 1. Macroseismic intensity maps for the earthquakes that occurred in northern Venezuela on June 24, 2026. Source: USGS

The present study focuses exclusively on modeling the second earthquake. The currently available evidence indicates that the reported impacts, particularly those observed along the coastal region of La Guaira State, are primarily attributable to the Mw 7.5 event rather than to the preceding Mw 7.2 earthquake. To illustrate the contrasting influence of the two earthquakes as a function of location, the following sections present simulations of the strong ground motion generated by the seismic doublet at two representative sites in Venezuela.

3.1 Significance of the Mw 7.5 Earthquake in La Guaira State

Although the earthquake sequence consisted of a seismic doublet and the first event reached a substantial magnitude of Mw 7.2, it produced only moderate shaking in La Guaira State and reportedly went unnoticed by a significant portion of the local population. Using the same modeling methodology described in detail later in this report, the seismic doublet was simulated at two locations separated by a considerable distance: Catia La Mar, in La Guaira State, located approximately 160 km from the epicentral area, and San Felipe, in Yaracuy State, located approximately 30 km from the epicenter. This comparison provides a preliminary illustration of the markedly different effects of the two earthquakes across different regions of Venezuela.

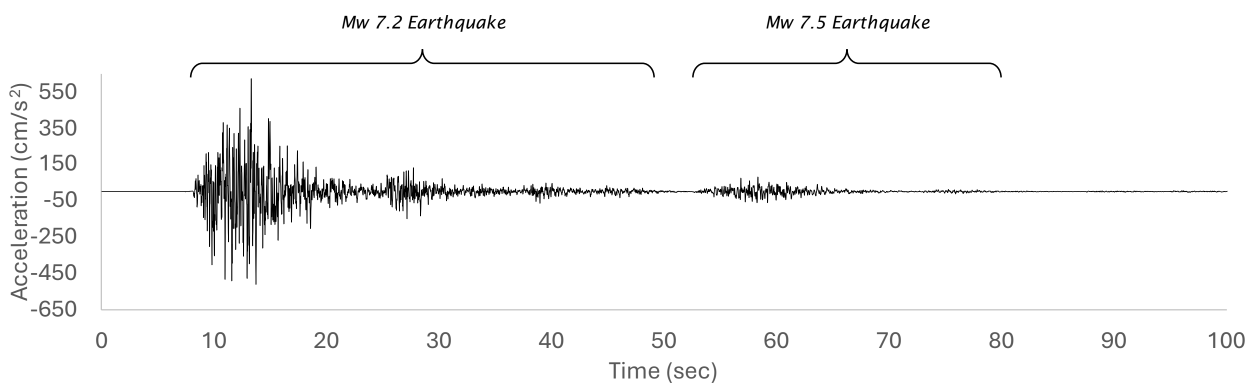

Figure 2. Simulated accelerograms for San Felipe, Yaracuy State.

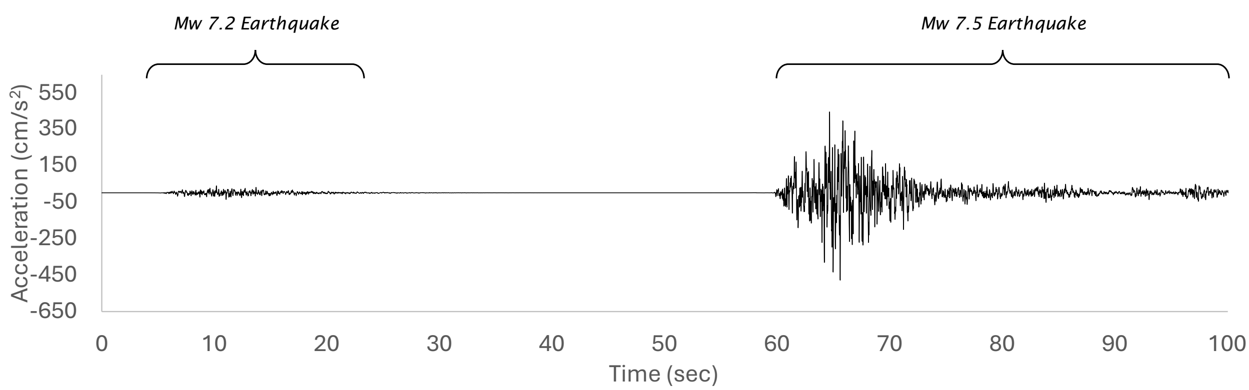

Figure 3. Simulated accelerograms for Catia La Mar, La Guaira State.

As shown in the simulated records, the ground motion in San Felipe is almost entirely dominated by the Mw 7.2 earthquake, whereas the ground motion in Catia La Mar is dominated by the Mw 7.5 event. Although the epicentral coordinates of the two earthquakes are nearly identical, the principal rupture areas are located in substantially different positions owing to the distinct rupture characteristics of each event. Consequently, there is no compelling evidence that the first earthquake contributed significantly to the damage observed in La Guaira State. For this reason, the analysis presented in this report focuses exclusively on the Mw 7.5 earthquake.

3.2 Characteristics of the Mw 7.5 Earthquake

The second earthquake, which occurred on the San Sebastián Fault, had a moment magnitude of Mw 7.5 and its rupture propagated with pronounced west-to-east directivity along a trajectory nearly parallel to the Venezuelan coastline. The event was a relatively shallow crustal strike-slip earthquake, with the largest fault slip concentrated offshore of La Guaira State. This source configuration is consistent with the concentration of the most severe observed impacts within the region, where the earthquake produced its most significant consequences.

The fundamental source parameters adopted in this study were obtained from data published by the USGS, including the earthquake magnitude, focal depth, epicentral coordinates, and focal mechanism solution (see Figure 4). The latter defines the rupture-plane geometry with strike = 86°, dip = 74°, and rake = -176°.

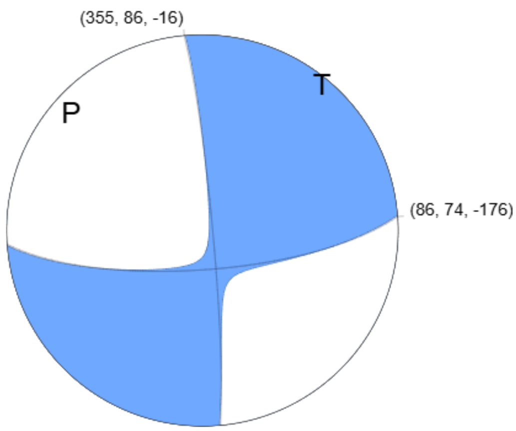

Figure 4. Focal mechanism solution for the Mw 7.5 earthquake. Source: USGS..

However, the rupture geometry inferred from the information published by the USGS is not entirely consistent with the apparent concentration of fault slip offshore of La Guaira State. This discrepancy is evident, for example, when compared with the permanent ground displacement estimates produced by the Copernicus Emergency Management Service of the European Union.

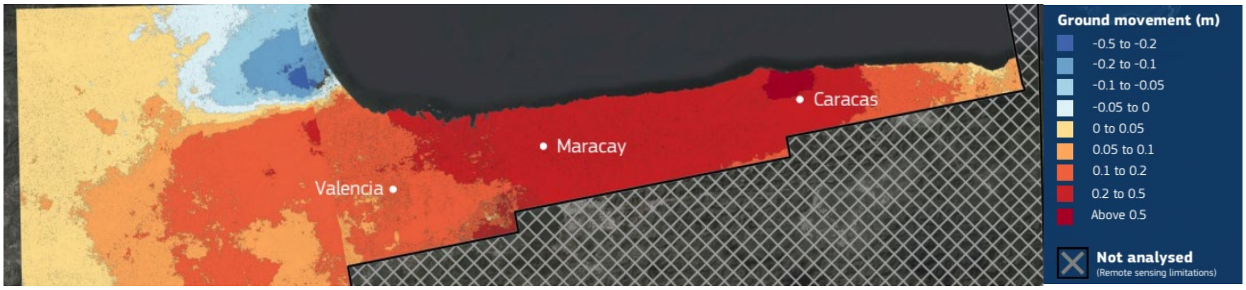

Figure 5. Permanent ground displacement associated with the June 24, 2026, Venezuela earthquakes, measured on June 25, 2026. Source: EU Copernicus.

An alternative rupture model has been proposed by the seismologist Bertrand Delouis (GEOAZUR) through inversion of the displacement field derived from observations recorded at seismic stations in Colombia and other Caribbean countries.[3] The resulting model is consistent with both the observed permanent ground displacements (Figure 5) and the pronounced concentration of damage in La Guaira State. Therefore, the present study adopts this rupture model for the strong ground motion simulations. Although the solution remains preliminary, it currently provides one of the most physically consistent interpretations of the rupture process and is in agreement with both the surface deformation patterns observed by Copernicus and the spatial distribution of the reported damage. The simulations presented herein should therefore be regarded as a first-order approximation that can be refined as additional observational data become available. Figure 6 summarizes the principal findings reported by Delouis regarding the rupture characteristics of the mainshock.

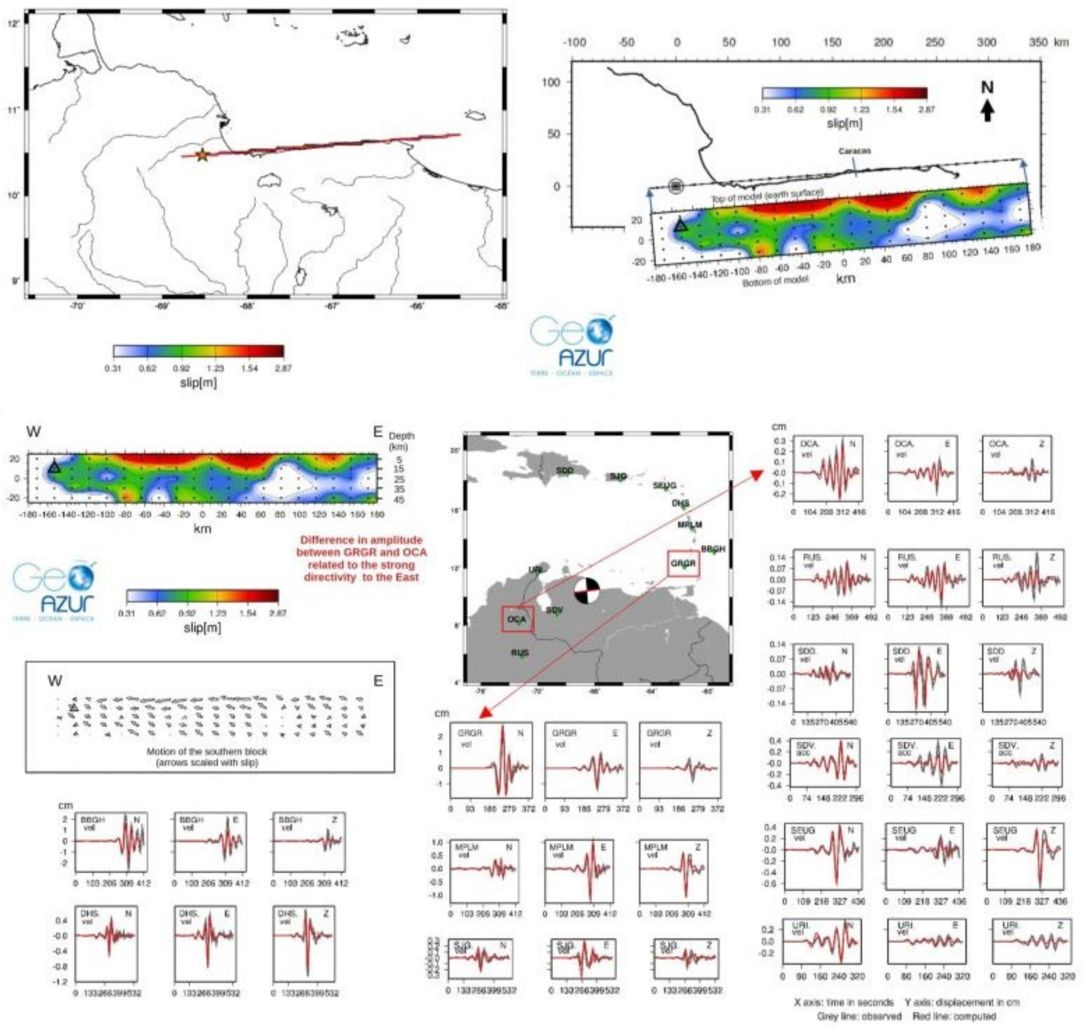

Figure 6. Schematic illustration of the slip inversion process used to determine the rupture characteristics. Source: Bertrand Delouis [4].

[3] At the time this report was prepared, no strong-motion recordings from within Venezuelan territory were available.

[4] Link to the publication: https://www.linkedin.com/posts/bertrand-delouis-30a532369_updated-slip-model-obtained-using-regional-share-7479113750709612544--VTi/?utm_source=share&utm_medium=member_android&rcm=ACoAAC7Bx14B7hQFn785BXRTKc_uzD-LWAGYCsM

3.3 Parameters adopted for the simulations

Based on the information described above, the earthquake source was modeled using the parameters summarized in Table 1.

Table 1. Parameters adopted for the rupture model.

Parameter	Value	Source
Epicentral coordinates (Lat, Lon – WGS 84)	-68.472, 10.4335	*USGS*
Magnitude (Mw)	7.5	*USGS*
Seismic moment (N-m)	2.24E+20	*USGS*
Depht (Km)	23	*USGS*
Strike (ϕ)	86	*USGS*
Dip (δ)	74	*USGS*
Rake (λ)	-176	*USGS*
Relative hypocenter location on the fault plane Dip direction	0.5	*Authors*
Relative hypocenter location on the fault plane. Strike direction	0.05	*Authors*
Relative location of the maximum fault slip on the fault plane. Dip direction	0.6	*Authors*
Relative location of the maximum fault slip on the fault plane. Strike direction	0.5	*Authors*
Aspect ratio of the rupture plane	9	*B. Delouis*
Rupture area (Km^2)	14,400	*B. Delouis*
Fault plane size along the strike direction (Km)	360	*B. Delouis*
Fault plane size along the dip direction (Km)	40	*B. Delouis*
Rupture propagation velocity (Km/s)	3.8	*B. Delouis*

The regional extent of the modeled rupture is presented in Figure 7. As shown, the simulated slip distribution is concentrated offshore of La Guaira State, consistent with both the seismological model and the observed damage patterns reported to date.

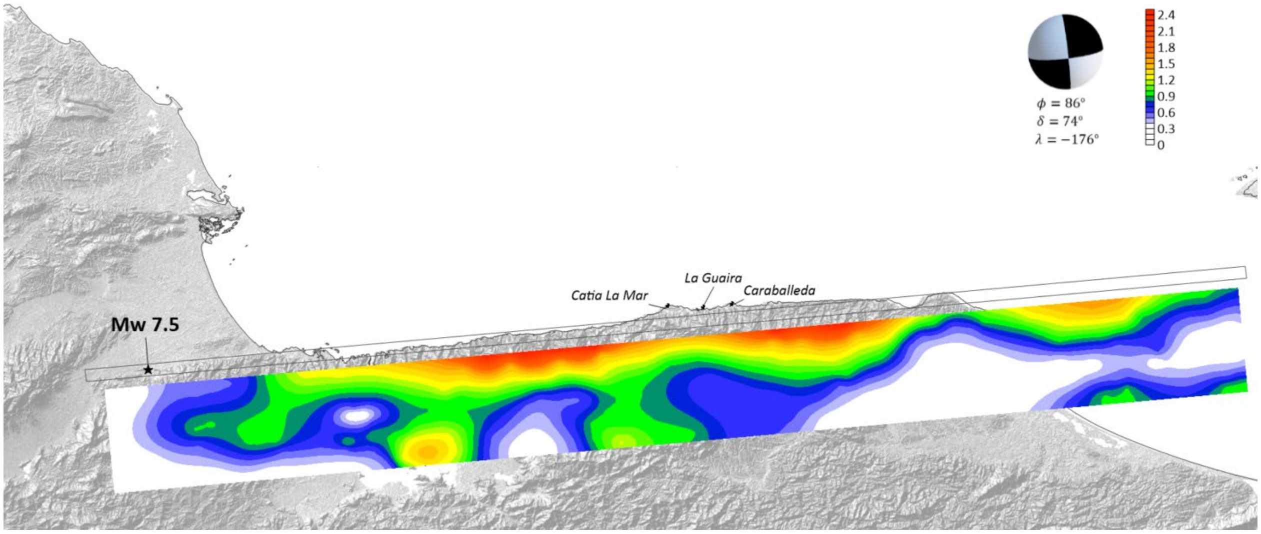

Figure 7. Simulated rupture model showing the concentration of fault slip offshore of La Guaira State. Slip is expressed in meters.

3.4 Regional strong ground motion

Based on the source characterization described above, the regional distribution of strong ground motion generated by the modeled earthquake was simulated throughout the study area. The simulations were performed using the simplified methodology proposed by Bernal et al. (2026) together with the reference Ground Motion Prediction Equation (GMPE) developed by Bernal and Cardona (2019). For illustrative purposes, the near-surface site conditions within the affected region were represented using the Vs30 parameter obtained from the USGS database. It should be emphasized that this information is included solely to provide a general description of the regional site conditions and does not constitute an evaluation of local site effects, which is presented separately in Section 5.

Figure 8 presents the contour map of the Peak Ground Acceleration (PGA) estimated for the simulated rupture. Overall, the regional distribution of ground-motion intensity is consistent with the observed damage patterns and provides a reasonable representation of the damage and loss assessment jointly developed by INGENIAR and ERN for the United Nations Office for Disaster Risk Reduction (UNDRR) [5].

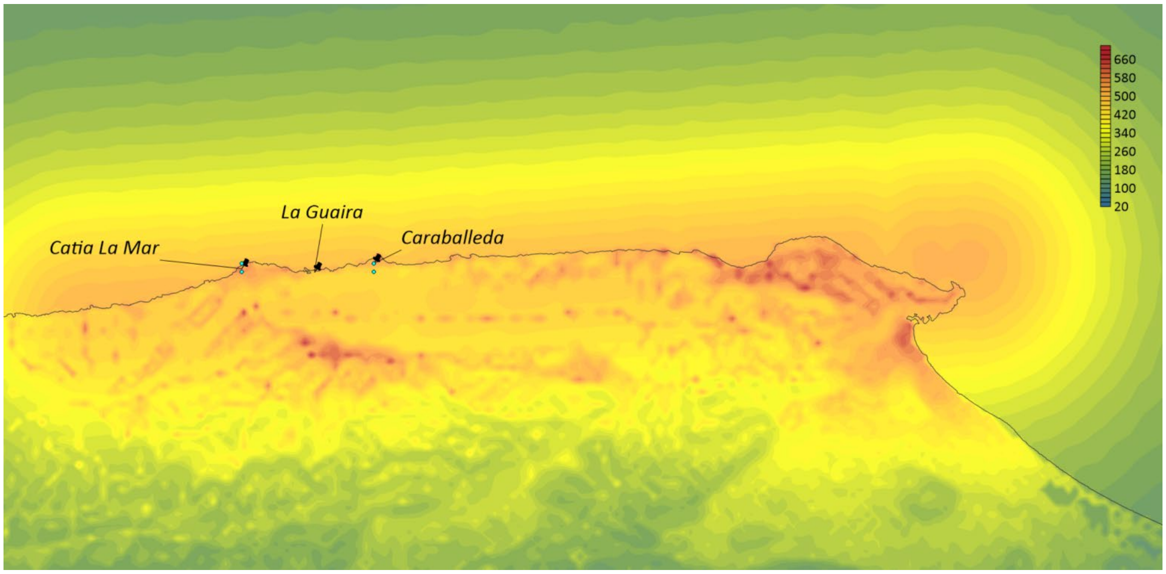

Figure 8. Spatial distribution of Peak Ground Acceleration (PGA) for the simulated rupture.

4 LOCAL ACCELEROGRAM SIMULATIONS

Given the apparent concentration of damage within the urban areas of La Guaira State, three representative locations were selected for detailed strong ground motion simulations: Catia La Mar, La Guaira, and Caraballeda. The simulations were carried out using the methodology proposed by Bernal et al. (2026), which enables the generation of physically realistic broadband strong-motion accelerograms whose frequency content is consistent with the rupture characteristics described in Section 3. In all cases, the simulated accelerograms correspond to the principal component of the ground motion. Consequently, the model is independent of the orientation of the recording axis.

[5] The report estimates direct economic losses of approximately USD 37 billion.

Figure 9 through Figure 11 present the simulated acceleration, velocity, and displacement time histories together with their corresponding response spectra. The simulated time histories exhibit pronounced velocity pulses associated with rupture directivity, consistent with the strong west-to-east propagation of the rupture and the forward-directivity effects toward the modeled sites. Most of the seismic energy is concentrated within relatively short time intervals for an earthquake of this magnitude, with the strongest shaking lasting less than approximately 10 seconds, followed by lower-intensity contributions generated by portions of the rupture located farther from the analyzed sites.

The resulting accelerograms represent physically consistent simulations of the expected strong ground motion for the modeled rupture scenario and are not intended to replace instrumental recordings, which are unavailable for this event. Their principal value lies in reproducing, on the basis of seismological and earthquake engineering principles, the temporal evolution of the ground motion, its frequency content, and the directivity-induced velocity pulses that characterize large earthquake ruptures.

Accordingly, these simulations provide a physically consistent explanation for the severity of the observed ground shaking and constitute valuable input for structural vulnerability assessments, seismic performance evaluations, calibration of design and analysis response spectra, and even for urban planning, not only from a prescriptive design perspective—as proposed in previous studies[6]—but also as a basis for land-use regulation, post-earthquake reconstruction, and long-term recovery planning.

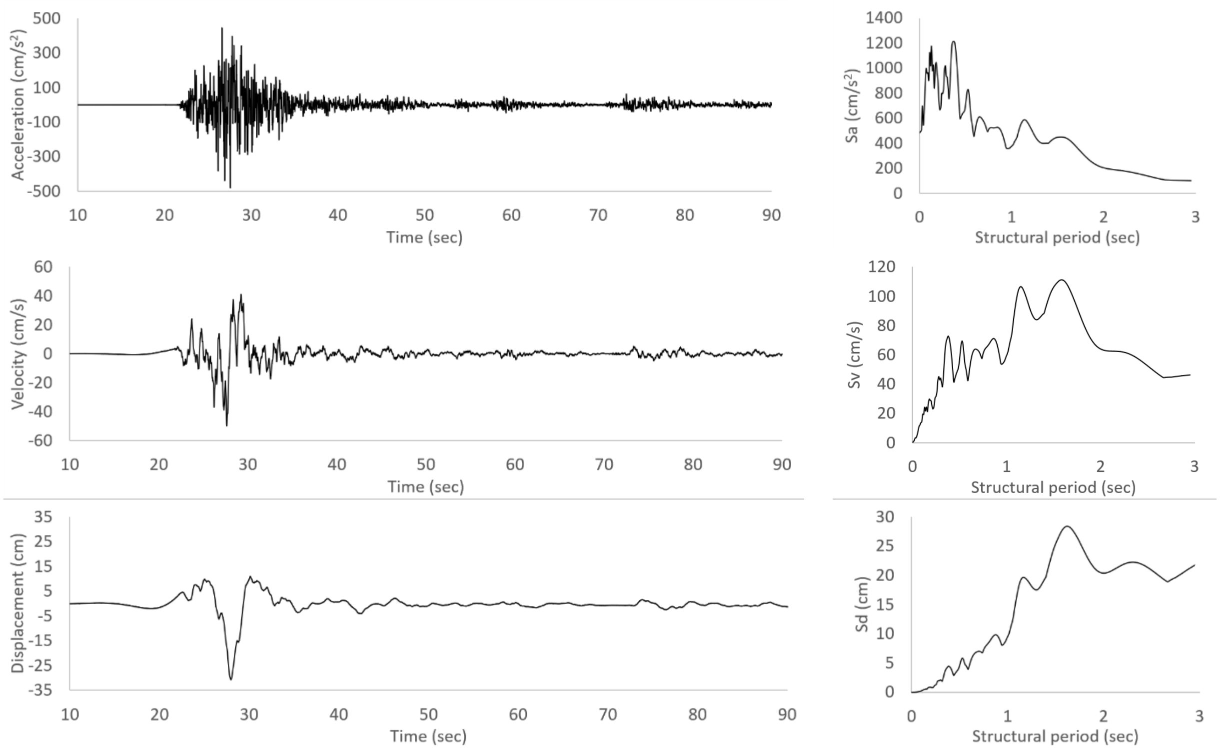

Figure 9. Simulated acceleration, velocity, and displacement time histories and corresponding response spectra for Catia La Mar.

[6] Disaster Risk Reduction in Urban Planning: A Case Study of Caraballeda Parish, Vargas State (Ketty C. Mendes).

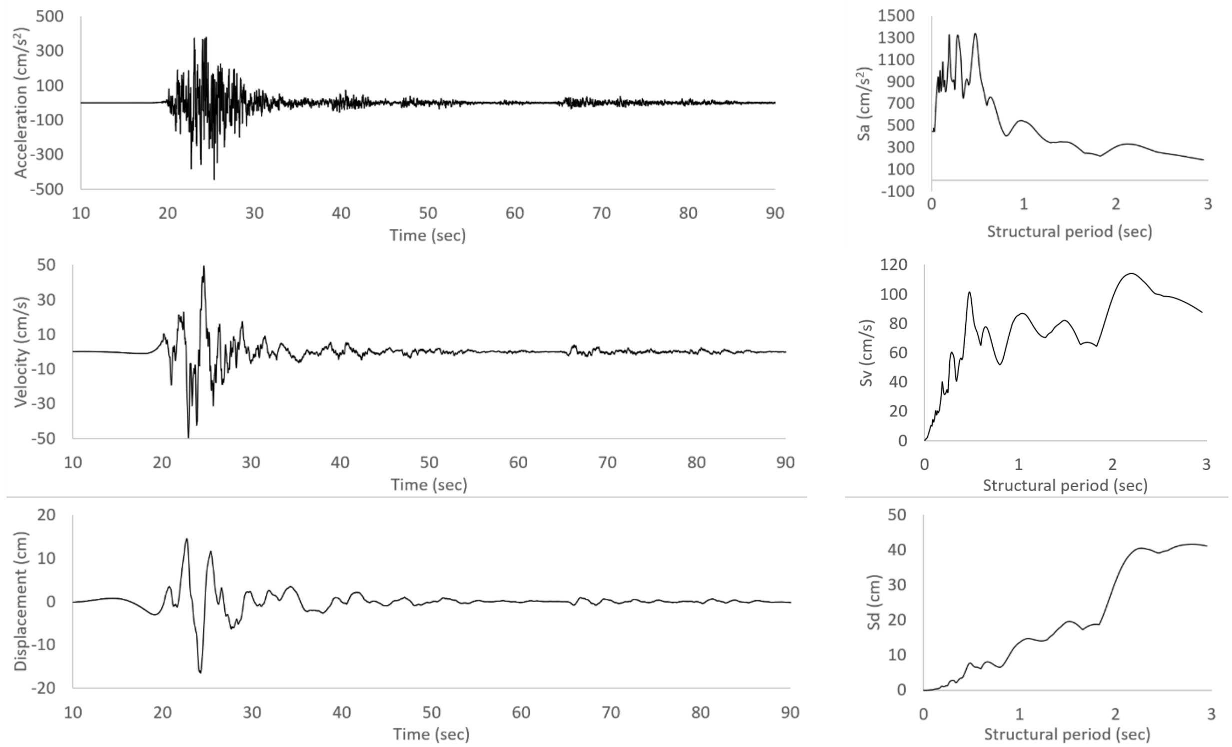

Figure 10. Simulated acceleration, velocity, and displacement time histories and corresponding response spectra for La Guaira.

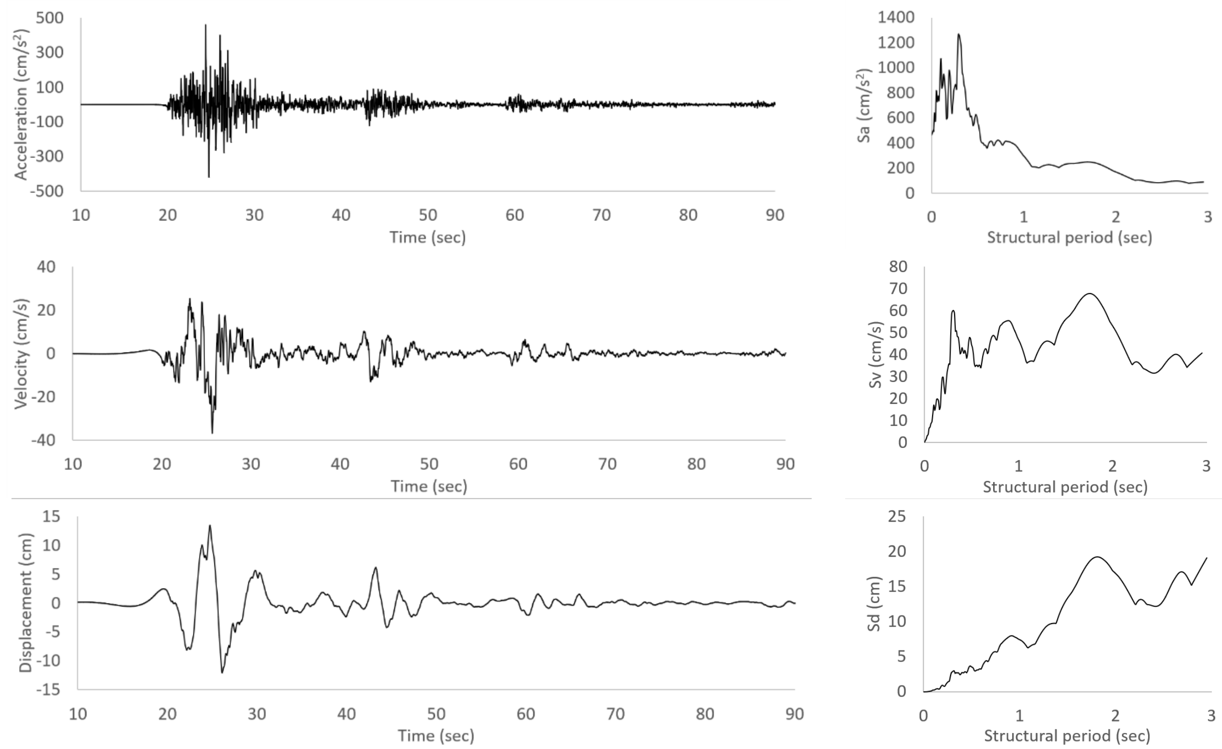

Figure 11. Simulated acceleration, velocity, and displacement time histories and corresponding response spectra for Caraballeda.

5 MODELING OF THE LOCAL RESPONSE OF ALLUVIAL DEPOSITS

It is well established that many urban areas along the Venezuelan Caribbean coast are founded on alluvial fans formed by sediments eroded from the Ávila Mountain Range and transported by rivers and streams draining toward the Caribbean Sea. Throughout history, these alluvial deposits have provided favorable conditions for human settlement and urban development.

The three locations analyzed in this study—Catia La Mar, La Guaira, and Caraballeda—are largely situated on these alluvial deposits, although urban development also extends onto the adjacent mountain slopes of the Ávila Range. The apparent correlation between the observed damage patterns and the dynamic response of these surficial deposits constitutes one of the principal hypotheses investigated in this section.

5.1 Available data

Among the study locations, Caraballeda has the most comprehensive geotechnical and geophysical information available regarding subsurface conditions and site response. Consequently, the detailed analyses presented herein focus on this location. Given the geological and geomorphological similarities among the study sites, the results are subsequently used as a proxy for the remaining locations.

The geological conditions of Caraballeda have been extensively investigated and are among the best characterized along the Venezuelan coast. Romero et al. (2006) presented a bedrock depth map derived from the interpretation of Bouguer gravity anomaly measurements acquired in Caraballeda and neighboring communities, including Tanaguarena, Macuto, and La Guaira. Their study indicates bedrock depths of up to approximately 450 m beneath the coastal plain (see Figure 12) and reports geophysical measurements of shear-wave velocity (Vs), which are summarized in Table 2.

The authors also report groundwater depths ranging from 5 to 10 m across the study area. In addition, the results indicate that, at depths greater than approximately 100 m, the alluvial deposits are sufficiently consolidated to be considered engineering bedrock (Vs > 800 m/s).

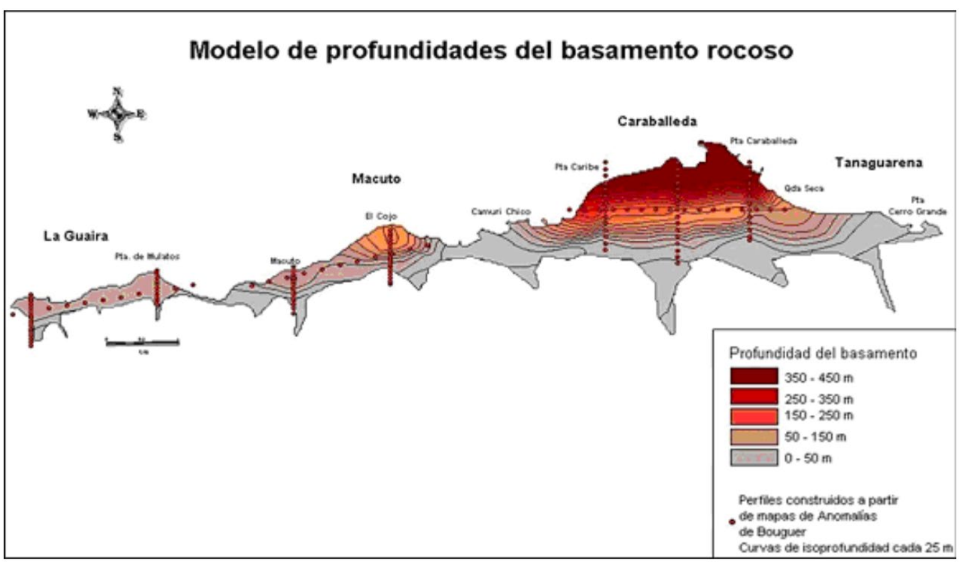

Figure 12. Bedrock depth model for Caraballeda. Source: Romero et al. (2006).

Table 2. Measured shear-wave velocity ranges within the Caraballeda alluvial deposits. Adapted by the authors from Romero et al. (2006).

Z (m)	Minimum Vs (m/s)	Maximum Vs (m/s)	Average (m/s)
50	215	400	307.5
100	425	570	497.5
> 100	> 800		

In turn, García et al. (2023) proposed a seismic microzonation of Caraballeda based on combinations of sediment thickness and average shear-wave velocity within the alluvial deposits. Their work also presents a representative geological cross-section of the alluvial fan, showing deposit thicknesses of up to approximately 400 m (see Figure 13), which served as the basis for defining planning zones for future urban development.

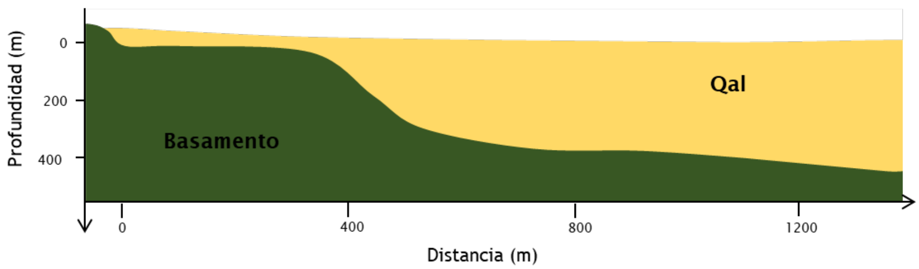

Figure 13. Geological cross-section through Caraballeda. Qal = alluvial fan deposits. Reproduced from García et al. (2023).

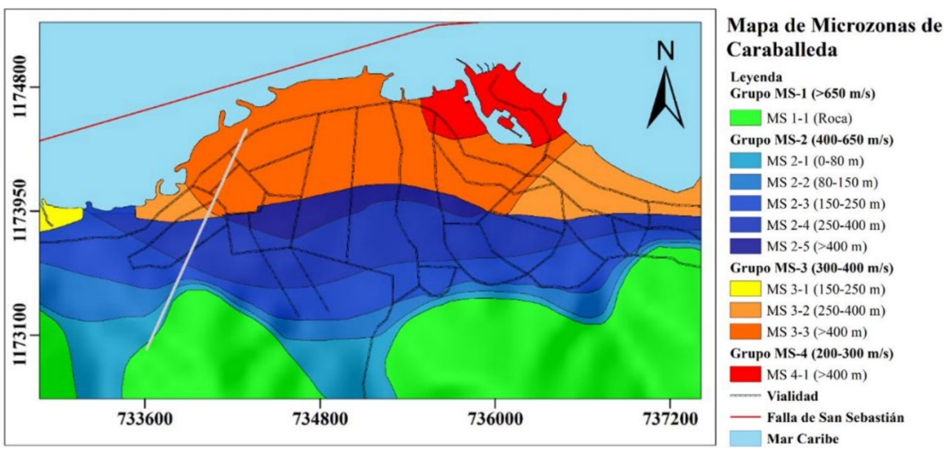

Figure 14. Seismic microzonation map of Caraballeda. Source: García et al. (2023).

5.2 Local site response model

Two representative stratigraphic profiles were developed to characterize the local geotechnical conditions: one with a total thickness of 50 m and another 100 m thick. Each profile was discretized into uniform 5-m-thick layers representing well-graded sand soil (SW). The average shear-wave velocity assigned to each layer was defined as a function of depth using the values summarized in Table 2. A groundwater table located 5 m below the ground surface was assumed for both profiles.

One-dimensional seismic wave propagation analyses were performed for both profiles using a non-linear method (linear equivalent method by Idriss and Seed (1968)). The average modulus reduction and damping relationships proposed by Seed et al. (1986) were assigned to all soil layers. Under small-strain conditions (i.e., maximum shear modulus), the computed fundamental periods of the modeled soil profiles are 1.0 s for the 50-m profile and 1.34 s for the 100-m profile.

The simulated accelerograms for the three study locations were propagated through both hypothetical soil profiles. Figure 15 presents the Fourier spectral transfer functions obtained for each profile using each of the simulated rock outcrop accelerograms as the incident input motion. Figure 16 shows the corresponding response spectral amplification ratios for both soil profiles.

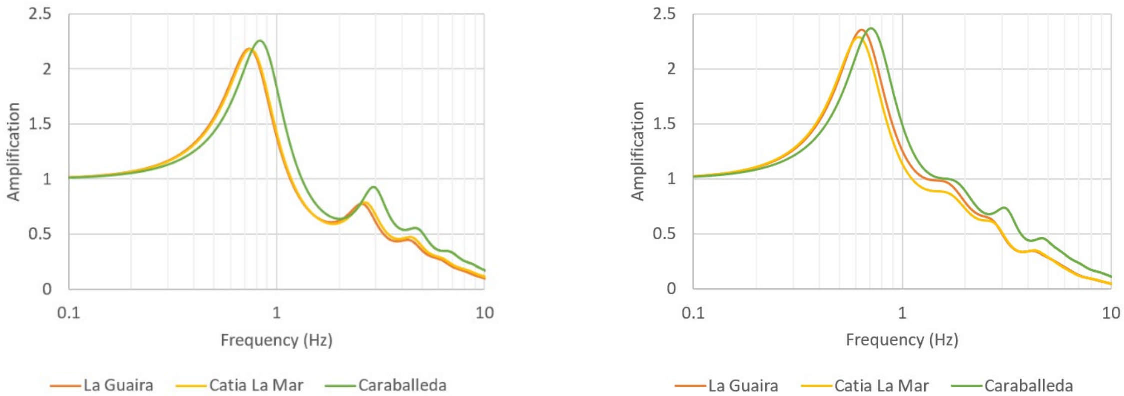

Figure 15. Modeled Fourier spectral transfer functions for the 50-m (left) and 100-m (right) soil profiles.

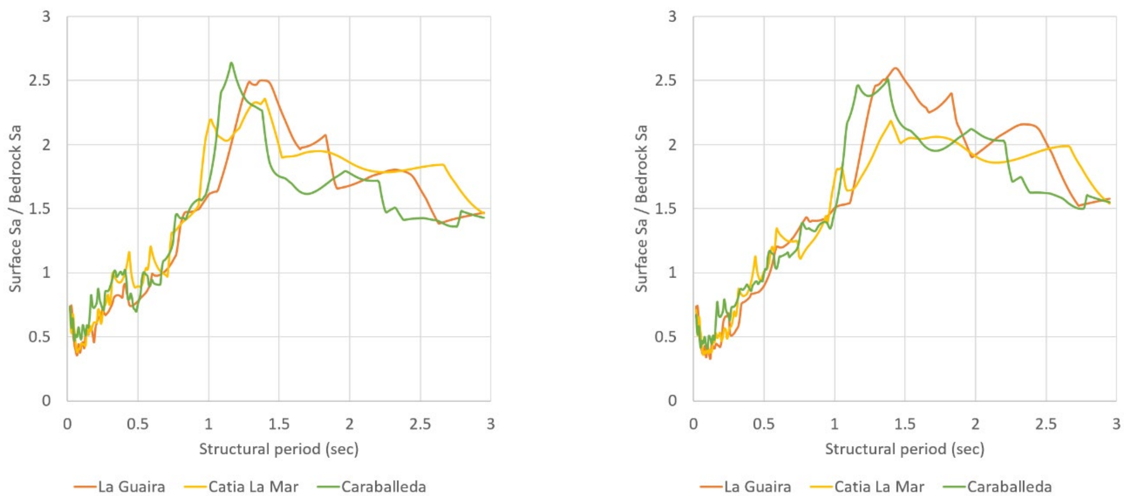

Figure 16. Response spectral amplification ratios for the 50-m (left) and 100-m (right) soil profiles.

The following figures present the simulated ground motions at the ground surface obtained from the one-dimensional wave propagation analyses performed for the 50-m-thick soil profile. The results include acceleration, velocity, and displacement time histories at the ground surface, together with their corresponding response spectra.

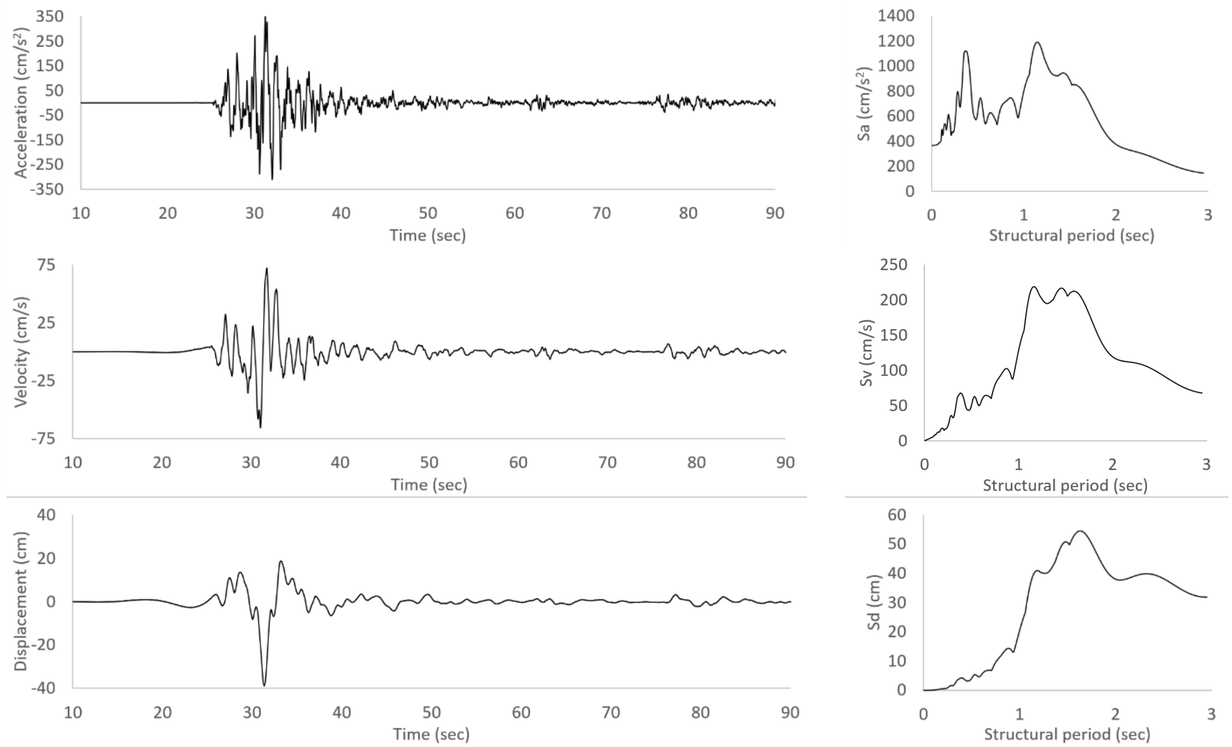

Figure 17. Simulated acceleration, velocity, and displacement time histories and corresponding response spectra at the ground surface in Catia La Mar, considering a 50-m-thick soil profile.

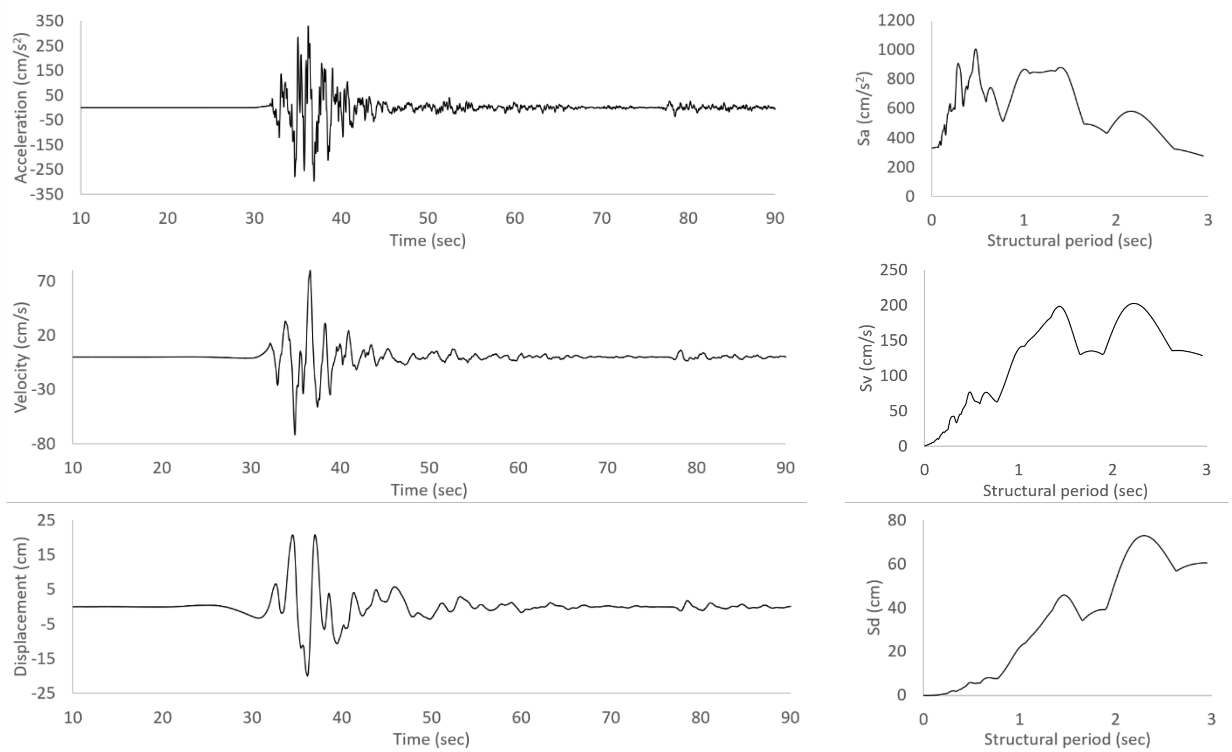

Figure 18. Simulated acceleration, velocity, and displacement time histories and corresponding response spectra at the ground surface in La Guaira, considering a 50-m-thick soil profile.

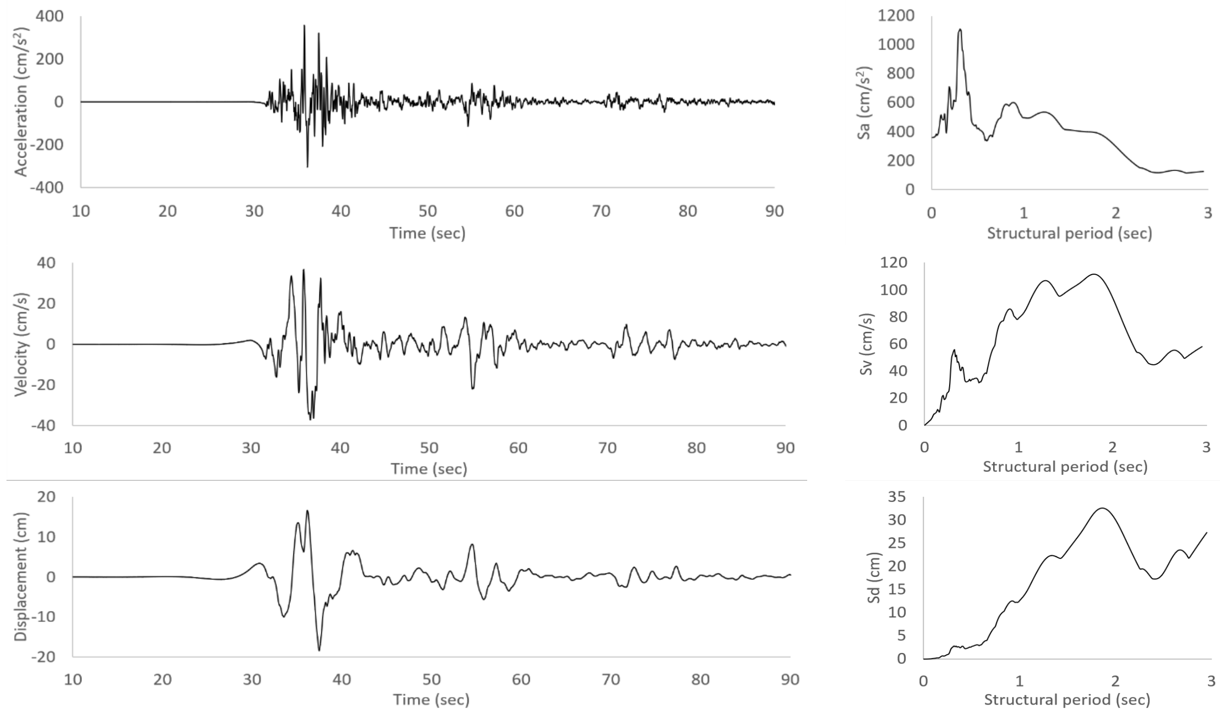

Figure 19. Simulated acceleration, velocity, and displacement time histories and corresponding response spectra at the ground surface in Caraballeda, considering a 50-m-thick soil profile.

The following figures present the simulated ground motions at the ground surface obtained from the one-dimensional wave propagation analyses performed for the 100-m-thick soil profile. The results include acceleration, velocity, and displacement time histories at the ground surface, together with their corresponding response spectra.

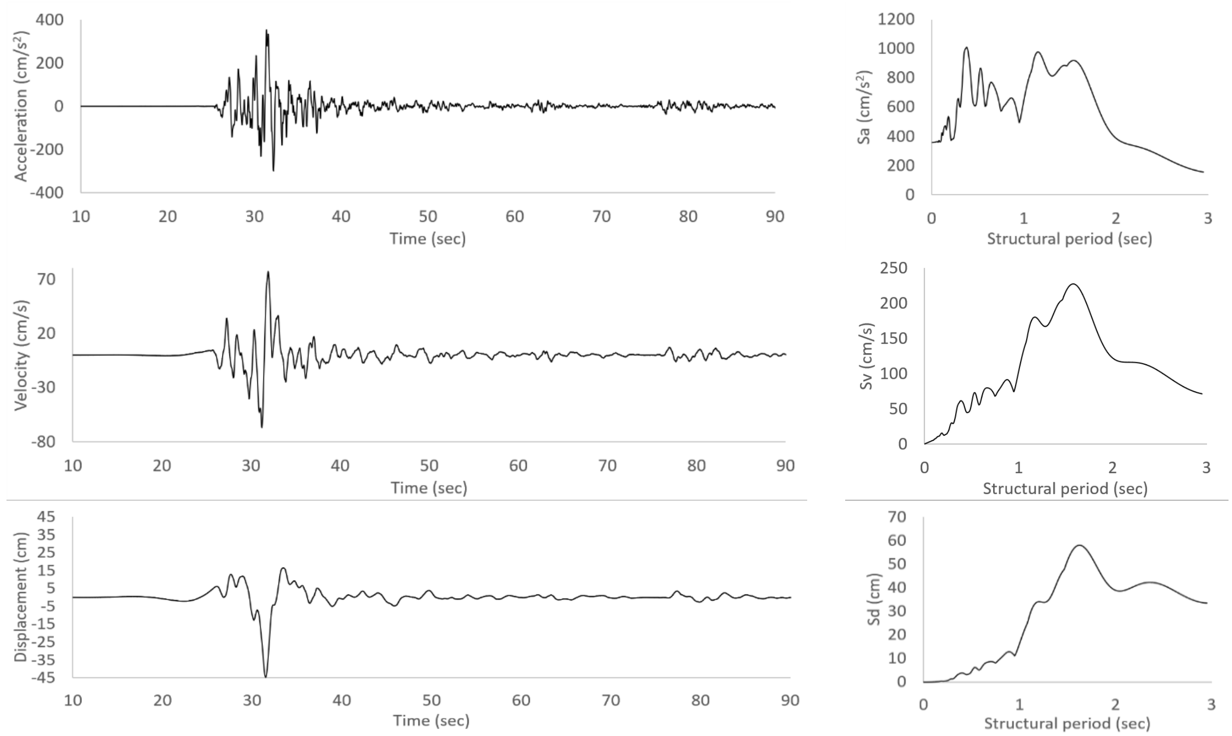

Figure 20. Simulated acceleration, velocity, and displacement time histories and corresponding response spectra at the ground surface in Catia La Mar, considering a 100-m-thick soil profile.

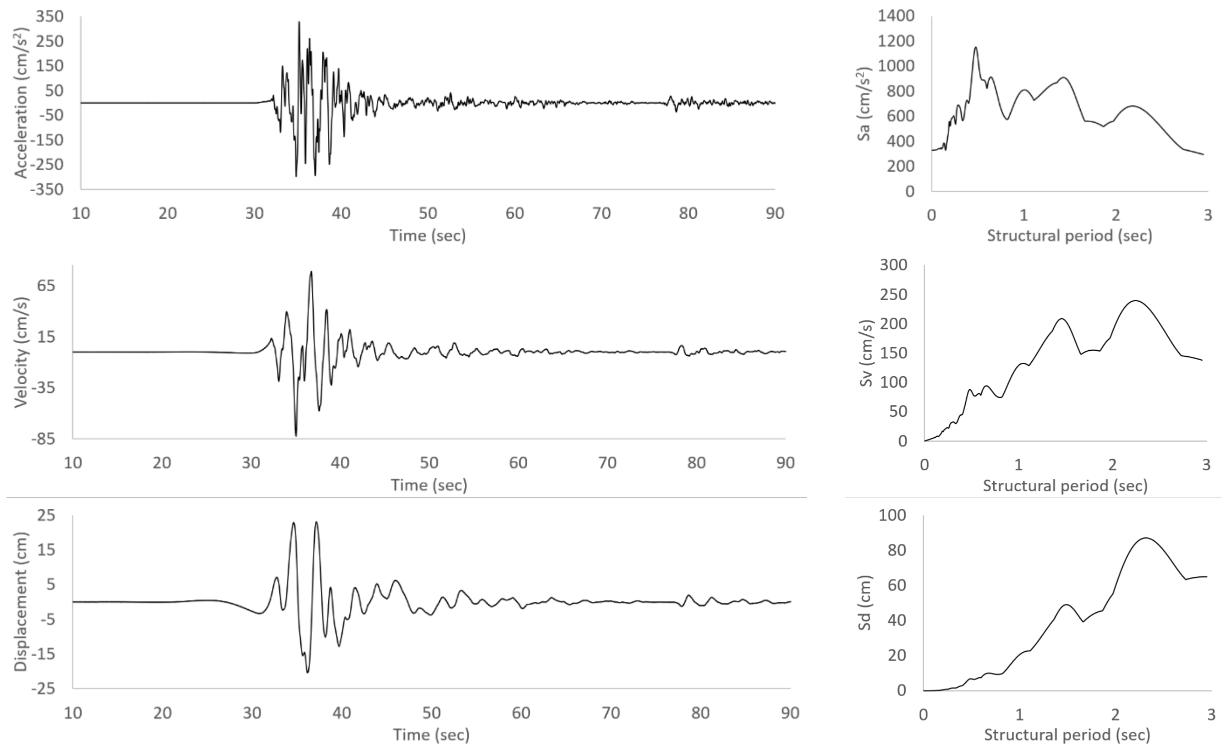

Figure 21. Simulated acceleration, velocity, and displacement time histories and corresponding response spectra at the ground surface in La Guaira, considering a 100-m-thick soil profile.

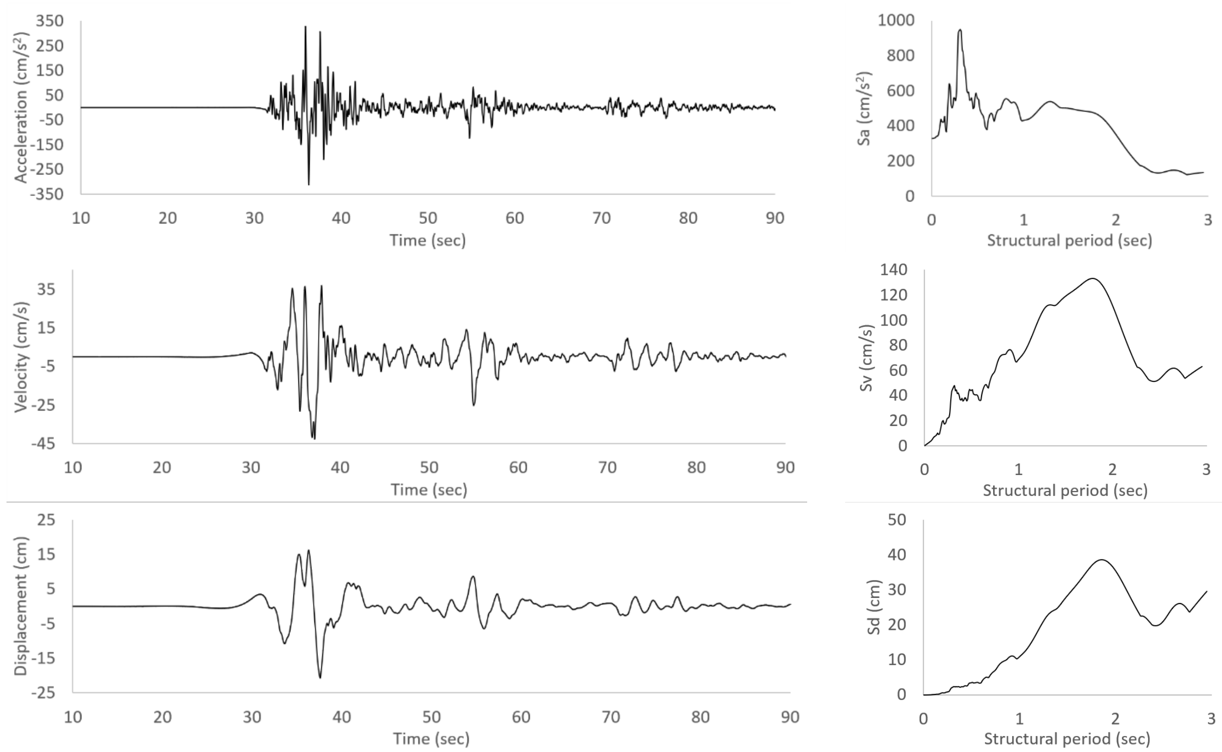

Figure 22. Simulated acceleration, velocity, and displacement time histories and corresponding response spectra at the ground surface in Caraballeda, considering a 100-m-thick soil profile.

5.3 Liquefaction potential

The superficial soils within the alluvial fans of La Guaira State are known to exhibit significant liquefaction potential given their geotechnical characteristics. Numerous locations within these deposits consist of saturated, poorly graded fine-grained granular soils, creating favorable conditions for the development of earthquake-induced liquefaction.

This section presents a set of reasonable assumptions regarding the geotechnical characteristics of the superficial alluvial deposits in La Guaira State to illustrate their liquefaction potential. This mechanism provides a plausible explanation for many of the damage patterns observed following the June 24, 2026, earthquake. The analysis considers a hypothetical layer of saturated granular soil located at a depth of 10 m, with an assumed dry unit weight of 19 kN/m³, representative of dense sand, as reported by Romero et al. (2006). Table 3 summarizes the assumed geotechnical parameters adopted for the liquefaction assessment.

Table 3. Assumed geotechnical parameters for the liquefaction assessment.

Variable	Unit	Value
Groundwater table depth	*m*	5
Dry unit weight	KN/m^3	19
Saturated unit weight	KN/m^3	22
Pore water pressure	*KPa*	50
Vertical stress	*KPa*	205
Effective vertical stress	*KPa*	155

The approximate method proposed by Andrus et al. (2003) was employed to estimate the critical peak ground acceleration required to trigger liquefaction in the assumed soil profile. The method provides the critical resistance ratio (CRR) for earthquakes of Mw 7.5; consequently, no magnitude scaling factor was required because the magnitude of the modeled earthquake coincides with the reference magnitude of the procedure. In the method proposed by Andrus et al. (2003), soil stiffness is expressed in terms of shear-wave velocity therefore the analysis was referenced to the soil groups defined in the Caraballeda seismic microzonation developed by García et al. (2023) (see Figure 14). The corresponding results are summarized in Table 4.

Table 4. Critical resistance ratio (CRR) and critical peak ground acceleration for the Caraballeda soil groups defined by García et al. (2023)[7].

Variable			Group 4 (200 m/s)	Group 3 (300 m/s)	Group 2 (400 m/s)
Critical resistance ratio	$CRR_{7.5}$	-	0.111	0.201	0.378
Critical peak ground acceleration	$\boldsymbol{PGA_{crit}}$	$\boldsymbol{cm/s^2}$	**139**	**252**	**475**

As indicated by the results, the zones closest to the coastline, where the soils exhibit the lowest stiffness, have a very high liquefaction potential. The estimated critical accelerations would have been substantially exceeded during the ground shaking generated by the June 24, 2026, earthquake in La Guaira State. This

[7] Soil Group 1 of the Caraballeda seismic microzonation was not included because it corresponds to areas where bedrock crops out.

finding provides a plausible explanation for many of the observed failures affecting buildings and infrastructure, particularly overturning, differential settlement, and, in some cases, sudden structural collapse in areas adjacent to the coastline.

6 CONCLUSIONS

Although the simulations presented herein should be refined as additional seismological and instrumental data become available, they provide a technically sound first-order approximation for understanding the earthquake, supporting subsequent investigations, and informing post-earthquake reconstruction and disaster risk reduction efforts. The principal conclusions of this study are summarized below.

1. The Mw 7.5 earthquake was the primary cause of the damage observed in La Guaira State.

Although the seismic sequence consisted of a doublet comprising Mw 7.2 and Mw 7.5 earthquakes, the strong ground motion simulations indicate that the seismic demand along the central Venezuelan coast was controlled primarily by the Mw 7.5 event that occurred on the San Sebastián Fault. The rupture geometry, its location offshore of La Guaira State, and its west-to-east rupture propagation explain the spatial concentration of the observed damage and suggest that the precursor event made little, if any, significant contribution to the impacts documented in this region.

2. The rupture exhibited characteristics favorable for generating severe strong ground motion dominated by rupture directivity effects

The simulations indicate that the rupture generated pronounced velocity pulses characteristic of earthquakes exhibiting strong forward directivity, concentrating a substantial portion of the released seismic energy within relatively short time intervals. This behavior produced unusually high seismic demands at intermediate and long vibration periods, exceeding those typically expected for a conventional earthquake of similar magnitude and source-to-site distance. Rupture directivity therefore appears to have been one of the principal mechanisms controlling the severity of the ground shaking along the central Venezuelan coast.

3. The simulations provide a consistent representation of the characteristics of an exceptional earthquake.

The rupture associated with the second earthquake of June 24, 2026, was unusually extensive for an Mw 7.5 event, with relatively moderate fault slip, generally less than 2 m, concentrated offshore of La Guaira State rather than in the vicinity of the hypocenter. This rupture configuration generated exceptionally high shaking intensities and severe damage more than 150 km from the epicenter, far exceeding the levels predicted by conventional strong ground motion models, which would typically estimate PGA values of approximately 0.05–0.07 g at such distances. Both the simulated ground motions and the observed damage demonstrate that parameters such as the spatial distribution of fault slip and rupture propagation can play a decisive role in earthquake consequences, despite receiving little or no explicit consideration in conventional seismic hazard and risk assessments. This event underscores the need to strengthen earthquake monitoring and characterization systems while advancing current ground-motion simulation methodologies to adequately capture such exceptional rupture processes.

4. Regional seismic demand reached exceptionally high levels for the tectonic setting of northern Venezuela.

The strong ground motion simulations indicate shaking intensities consistent with an extreme seismic scenario for the region. The concentration of fault slip offshore of La Guaira State produced the highest seismic demands directly beneath the most densely populated urban areas along the central coast, creating an unfavorable coincidence between the earthquake source and the existing exposure. The resulting spatial distribution of seismic demand is consistent with both the reported damage patterns and the preliminary economic loss estimates developed for this event.

5. The alluvial deposits along the central Venezuelan coast provide conditions conducive to significant local site amplification.

The one-dimensional site response analyses performed for representative soil profiles with thicknesses of 50 m and 100 m demonstrate substantial modification of the incoming ground motion by the alluvial deposits underlying much of the coastal plain in La Guaira State. The simulations show pronounced spectral amplification concentrated around the fundamental periods of the deposits, increasing the seismic demand at the ground surface relative to engineering bedrock conditions and providing a consistent explanation for the concentration of damage observed across the region's alluvial fans.

6. The simulated strong ground motion provides a consistent explanation for the observed damage.

Very severe seismic demands are identified for buildings between 10 and 20 stories in height, associated with a frequency content controlled by the pronounced rupture directivity and exacerbated by the soft soils of the alluvial fans, which promote amplification at structural periods longer than 0.8 s and exhibit significant liquefaction potential that was likely exceeded at numerous locations. Likewise, the short-period ground accelerations, with PGA values ranging from 0.45 to 0.50 g at engineering bedrock and from 0.30 to 0.35 g at the ground surface, explain the observed damage to low-rise buildings. Although this damage is distributed throughout the building stock of La Guaira State, its spatial variability is consistent with local differences in structural vulnerability, near-surface geotechnical conditions, and topographic effects that were not considered in this study. Overall, the observed damage is reasonably consistent with the seismic intensities simulated in this study.

7. The interaction between rupture directivity and local site effects created particularly critical conditions for structures with intermediate and long natural periods.

The coincidence between the velocity pulses generated by the rupture and the predominant vibration periods associated with the deep alluvial deposits produced significant amplification of the response spectral ordinates within the 1–2 s period range. This condition resulted in particularly severe seismic demands for mid-rise and high-rise buildings, as well as for certain types of infrastructure, demonstrating that the intensity of the ground motion cannot be adequately characterized solely by simplified parameters such as PGA or spectral acceleration ordinates.

8. The findings support the need to revisit seismic design criteria, seismic microzonation, urban planning, and resilient reconstruction strategies for the central Venezuelan coast.

The combination of a large rupture, pronounced rupture directivity, deep alluvial deposits, and significant liquefaction susceptibility demonstrates that the local seismic hazard may substantially exceed the conditions predicted by simplified regional approaches. These findings support the need to review and update the design response spectra currently adopted for these areas, strengthen seismic microzonation studies, and incorporate land-use planning criteria that may even restrict or condition future urban development in areas highly susceptible to ground-motion amplification and associated hazards such as soil liquefaction.

MODELLING SOFTWARE

All simulations presented in this study were performed using *SMA – Strong Motion Analyst* (Gabriel Bernal, 2014). The software is freely available and can be downloaded from: https://ingeniar-risk.com/documentos/setupSMA_2026

GROUND MOTION SIMULATION DATA AND LICENSE

In the course of this study, additional strong ground motion simulations were generated for other locations throughout Venezuela, including simulations of the Mw 7.2 and Mw 7.5 earthquakes that were not included in this report. The complete set of simulated strong ground motions is released under the Creative Commons Attribution-ShareAlike 4.0 International (CC BY-SA 4.0) license.

Any individual or organization is hereby granted permission to copy, distribute, share, adapt, modify, and use these data for any purpose, including academic, technical, commercial, and research applications, provided that appropriate credit is given to the original authors and that any derivative works are distributed under the same CC BY-SA 4.0 license.

The full license text is available at: https://creativecommons.org/licenses/by-sa/4.0/

The data are provided "as is", without warranties or representations of any kind, either express or implied. The authors and participating institutions assume no responsibility or liability for any damages, losses, decisions, or other consequences arising from the use or interpretation of these data.

Data download:

http://ingeniar-risk.com/documentos/Venezuela%202026%20Ground%20Motion%20Simulations.zip

REFERENCES

Andrus, R.D., Stokoe, K.H., Chung, R.M., Juang, C.H., and Li, J.P. (2003). Guidelines for Evaluating Liquefaction Resistance Using Shear Wave Velocity Measurements. Report FHWA-RD-99-156, Federal Highway Administration (FHWA).

Bernal, G., Cardona, O.D. (2019). Ajuste de un Modelo de Espectro de Fuente y sus Aplicaciones en la Modelación de la Amenaza Sísmica y el Campo Cercano en Colombia. Memorias del IX Congreso Nacional de Ingeniería Sísmica, Cali, Colombia.

Bernal, G., Cardona, O.D., Ordaz, M. (2026). Simplified and Highly Efficient Simulation of Broadband Strong-Motion Accelerograms. Proceedings of the 18th European Conference on Earthquake Engineering. Berlin, Germany.

García, L., Rondón, F., Crasto, N., & Schmitz, M. (2023). Microzonas sísmicas preliminares del Estado La Guaira, en base a evaluación de Vs30, estudios gravimétricos y espesor de sedimentos. En: II Congreso Venezolano de Geociencias, Universidad Central de Venezuela, Caracas, marzo de 2023.

Idriss, M. I. y Seed, H. B. (1968). Seismic Response of Horizontal Soil Layers. Journal of the Soil Mechanics and Foundations Division, ASCE, Vol 94, N° SM4, Julio 1968.

Mendes A., Ketty C. (2013). La reducción del riesgo de desastres en la planificación urbana. Caso de estudio: la parroquia Caraballeda, estado Vargas, Venezuela. Tesis de Maestría en Planificación Urbana. Facultad de Arquitectura y Urbanismo, Universidad Central de Venezuela, Caracas, Venezuela.

Salgado, M.A., Bernal, G., Gayay, O., Ordaz, M., Cardona, O.D. (2026). Estimación analítica de daños ocasionados por los terremotos del 24 de junio de 2026 en Venezuela. Reporte especial de UNDRR. INGENIAR y ERN.

Romero, M., Cragno, A., Schmitz, M., y Ambrosio, R. (2006). Caracterización de suelos con métodos geofísicos en La Guaira, Macuto, Caraballeda y Tanaguarena, Estado Vargas, Venezuela. Revista Técnica de la Facultad de Ingeniería, Universidad del Zulia, 29(1), 3–15.

Seed, H.B., Wong, R.T., Idriss, I.M., and Tokimatsu, K. (1986). Moduli and Damping Factors for Dynamic Analyses of Cohesionless Soils. Journal of Geotechnical Engineering, ASCE, 112(11), 1016–1032.